Catalysis Letters (2019) 149:942–949
https://doi.org/10.1007/s10562-019-02687-w

The Propylene Oxide Rearrangement Catalyzed by the Lewis Acid Sites of ZSM-5 Catalyst with Controllable Surface Acidity

Mengnan Liang[1] · **Xiangshuai Zhu**[1] · **Weihua Ma**[1]

Received: 2 November 2018 / Accepted: 23 January 2019 / Published online: 7 February 2019
© Springer Science+Business Media, LLC, part of Springer Nature 2019

Abstract

The rearrangement of propylene oxide is greatly affected by the acidity of the catalyst. ZSM-5 zeolite with easily regulated surface acidity was used to catalyze the reaction with propionaldehyde as main product. The difference in the ratio of silica to alumina resulted in significant changes in the acidity. The results show that the ratio of the amount of Lewis acid sites (LAS) to the amount of Brønsted acid sites (BAS) has a great positive influence on the catalytic performance. When the ratio of silica to alumina reaches 50, the ratio of the LAS to BAS reaches the maximum value of 18.6, the catalytic performance is excellent. The in-situ diffuse reflectance Fourier transform infrared spectroscopy (DRIFTS) was employed to study the adsorption and reaction behavior of propylene oxide on the ZSM-5 catalyst. Results showed that the epoxy ring of propylene oxide first adsorbs on the Lewis acid site (Al atom with empty electron orbital) of ZSM-5 catalyst to form an intermediate with the bond between C=O and C–O which then converts to the propionaldehyde. The Lewis acid sites is of great importance for the reaction.

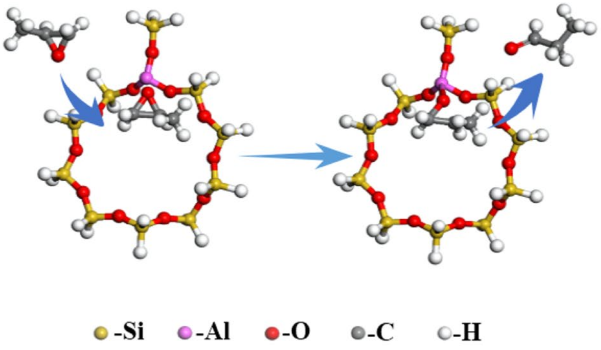

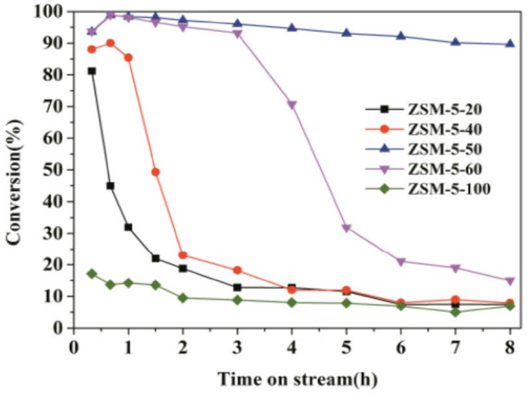

Keywords Propylene oxide rearrangement · Propionaldehyde · ZSM-5 zeolite · Silica/alumina ratio · Lewis acid site

1 Introduction

Epoxide is an important intermediate in organic synthesis because epoxy ring can be easily converted into chemicals with functional groups such as aldehydes, ketones, or alcohols [1–3]. As a kind of important epoxides, propylene oxide, due to its thermodynamic unstable three-membered epoxy ring, is prone to ring-opening reaction at high temperature or in the presence of a catalyst [4, 5]. The current research on the ring-opening reaction of propylene oxide mainly focuses on two aspects. Firstly, propylene oxide

---

Mengnan Liang and Xiangshuai Zhu have contributed equally to this work.

Electronic supplementary material The online version of this article (https://doi.org/10.1007/s10562-019-02687-w) contains supplementary material, which is available to authorized users.

✉ Weihua Ma
maweihuacn@163.com

[1] School of Chemical Engineering, Nanjing University of Science and Technology, Nanjing 210094, Jiangsu, People's Republic of China

undergoes ring-opening reaction to produce allyl alcohol, propionaldehyde, acetone, propanol and other products in the presence of catalyst [6–9]. Wang et al. prepared a hollow lithium phosphate catalyst for catalytic rearrangement of propylene oxide, which has high catalytic activity and high selectivity to allyl alcohol [4]. Secondly, the epoxy ring of propylene oxide reacts with carbon dioxide to form carbonates or form polymers with other epoxy compounds [10–12].

For the rearrangement of epoxides, the product distribution is determined by the acidity and alkalinity of catalyst, and is also affected by the migratory aptitude of the substituents on the epoxide group [13, 14]. Many researchers had done a lot of work on the rearrangement of propylene oxide, and it was found that when acid–base bifunctional catalyst was used, the main product was allyl alcohol, and when acidic catalyst was used, the product usually was propionaldehyde or ketone [4, 7, 15].

Zeolites as a catalyst with easily regulated surface acidity have been reported by some researchers to catalyze the epoxides rearrangement [16, 17]. For example, some researchers have used zeolites as catalysts in the rearrangement of macromolecular aliphatic epoxides, such as propylene oxide and 3-methyl-2,3-epoxybutane [18, 19]. Likewise, some results have been reported on the rearrangement of 1,2-alkane epoxides with long straight chain using zeolite as catalysts [5]. Since zeolite has a preponderance of acidity, it is more applicable to the acid catalyzed reaction [5, 20]. But for the propylene oxide rearrangement how the acidity affects the reaction and the product distribution is seldom investigated, and there was not enough evidence for the Lewis acid catalysis [18, 19]. In this paper we studied the effect of changes in the silica/alumina ratio on the acidity of ZSM-5 and the effect of acidity changes on propylene oxide rearrangement. Moreover, the catalysis of Lewis in propylene oxide rearrangement was confirmed and the mechanism of its rearrangement was proposed.

2 Experimental

2.1 Catalyst Preparation

ZSM-5 zeolites, with the SiO_2/Al_2O_3 molar ratios of 20, 40, 50, 60 and 100, were synthesized respectively according to the following procedure. First, 6.67 g of tetrapropylammonium hydroxide (TPAOH, 20% aqueous solution) was added dropwise to 13.211 g NaOH solution with mass percentage of 1%. The mixture was stirred for 0.5 h and then 31.78 g tetraethylorthosilicate (TEOS, AR) was added dropwise. The resulting mixture (I) was stirred for 1 h. Second, different amounts of $NaAlO_2$ (AR) were added to 13.211 g NaOH solution with mass percentage of 1%, the resulting mixture (II) was stirred for 1 h. Third, the resulting mixture (II) was added dropwise to mixture (I) with stirring and the resulting gel was stirred for 4 h. The molar composition of the gel was $1SiO_2$: xAl_2O_3: 0.043TPAOH: 0.046NaOH: $11.47H_2O$ ($x = 0.05$, 0.025, 0.02, 0.0167, 0.01). Finally, the gel was transferred to a 100 ml Teflon autoclave and reacted at 180 °C for 24 h. The product was washed and filtered repeatedly for several times, dried at 110 °C, and then calcined at 550 °C for 8 h in air to remove the templates. Samples with different ratios of silica to alumina are denoted as ZSM-5-x ($x = 20$, 40, 50, 60, 100).

2.2 Catalytic Performance Test

The performance test of ZSM-5-x catalysts was conducted in a fixed-bed reactor. 0.5 g ZSM-5-x catalyst was placed in a fixed-bed reactor with a diameter of 10 mm. The mixed gas of propylene oxide and N_2 was preheated at 200 °C and the reaction temperature was controlled at 300 °C. The weight hourly space velocity (WHSV) of propylene oxide was 19 h^{-1}. The products were analyzed by gas chromatography with an Agilent FF-AP capillary column.

2.3 Catalyst Characterization

X-ray powder diffraction (XRD) patterns were recorded on a Bruker D8 X-ray powder diffractometer with Cu Kα radiation ($\lambda = 1.5406$ Å). Fourier transform infrared spectroscopy (FTIR) of ZSM-5 was recorded on a Nicolet IS10 with pure KBr as background. A scanning electron microscopy (SEM, JSM6380) was performed to investigate the morphology of the samples. The actual ratio of silica to alumina in ZSM-5 was measured with an X-ray fluorescence (XRF, ThermoFisherARL). The pore structure and the apparent BET surface area of the samples were studied by nitrogen adsorption–desorption measurements at − 196 °C on ASAP 2460 MicroActive instrument. The acidity of the samples was measured by temperature-programmed desorption of ammonia (NH_3-TPD) on an automated chemisorption analyzer (Quantachrome Instruments) equipped with a thermal conductivity detector (TCD). The nature of acid sites was determined by pyridine adsorbed IR (Py-IR) spectroscopy on a Nicolet IS10 spectrometer. In situ DRIFTS measurements were performed on a Nicolet iS10 spectrometer equipped with an iZ10 Auxiliary Module, which consists of a liquid-N_2-cooled high-sensitivity MCT-A detector and a DRIFT cell (Spectra-Tech) with KBr windows. The sample [the mixture of KBr and the ZSM-5-50 catalyst (2:1)] was placed in an in situ DRIFT cell. All spectra were recorded with an accumulation of 4 scans and with a resolution of 4 cm^{-1}. The spectra began to be recorded as soon as the sample was heated in pure N_2 with flow of 10 ml/min. When the temperature reached the set value 300 °C, propylene oxide was introduced into the cell by a peristaltic pump. The fresh and used catalysts were characterized by thermogravimetric analysis (TG, Mettler-Toledo TGA/SDTA851e) at the rate of 10 °C/min in air (100 ml/min) atmosphere.

3 Results and Discussion

3.1 Catalyst Characterization

The X-ray diffraction patterns of ZSM-5 with silica/alumina molar ratios of 20, 40, 50, 60 and 100 are presented in Fig. 1a. The XRD patterns of these catalysts match well with the standard ZSM-5 XRD patterns (JCPDS 00-044-0003). All samples have the typical characteristic patterns of MFI structure with peaks at 2θ of 7.9°, 8.8°, 23.1°, 23.9° and 24.3° [21]. Figure 1b shows the FTIR spectra of all samples in the range of 400–1500 cm^{-1}. The peak at 544 cm^{-1} corresponds to the vibration of the double five-membered ring unit and the peak at 1232 cm^{-1} corresponds to the asymmetrical stretching vibration of MFI framework structure [22]. These two characteristic peaks also prove that all samples belong to the MFI configuration. The bands at 796 cm^{-1} and 1091 cm^{-1} are attributed to the symmetrical and antisymmetrical vibration of [SiO_4] units, respectively [23]. In addition, according to the SEM results (see supporting information Fig. S1), all samples are about 10 μm in size.

Low temperature N_2 adsorption–desorption experiments were performed to investigate the changes in the textural properties of all samples. The isotherms of all samples are shown in Fig. 2. Great adsorption amount at low relative pressure ($p/p_0 < 0.05$) for all the samples evidences the microporous structure of zeolite [24, 25]. Moreover, there is hysteresis loop in the isotherms of ZSM-5-20 and ZSM-5-100, indicating that the presence of mesopores which may be due to particle packing in the zeolite [25]. The pore size distribution of the sample was obtained by the Horvath–Kawazoe method. As shown in Fig. 2, all of the samples have similar pore size distributions, and the pore sizes are all concentrated around 0.65 nm. The BET surface area, pore volume and micropore characteristics are shown in Table 1. The BET surface area and the total pore volume of all samples are about 300 m^2/g and 0.17 cm^3/g, respectively. ZSM-5-50 has the largest BET surface area and total pore volume, 307.03 m^2/g and 0.176 cm^3/g, respectively. In addition, as the ratio of silica to alumina increases, the external specific surface area of all samples increases.

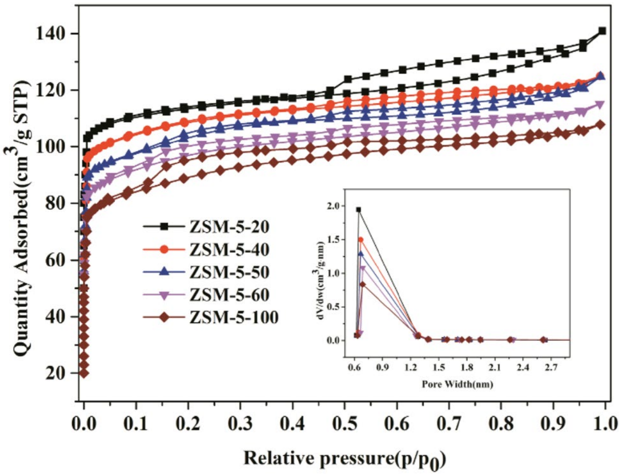

Fig. 2 N_2 adsorption–desorption isotherms (inset: pore size distribution deduced from the Horvath–Kawazoe method)

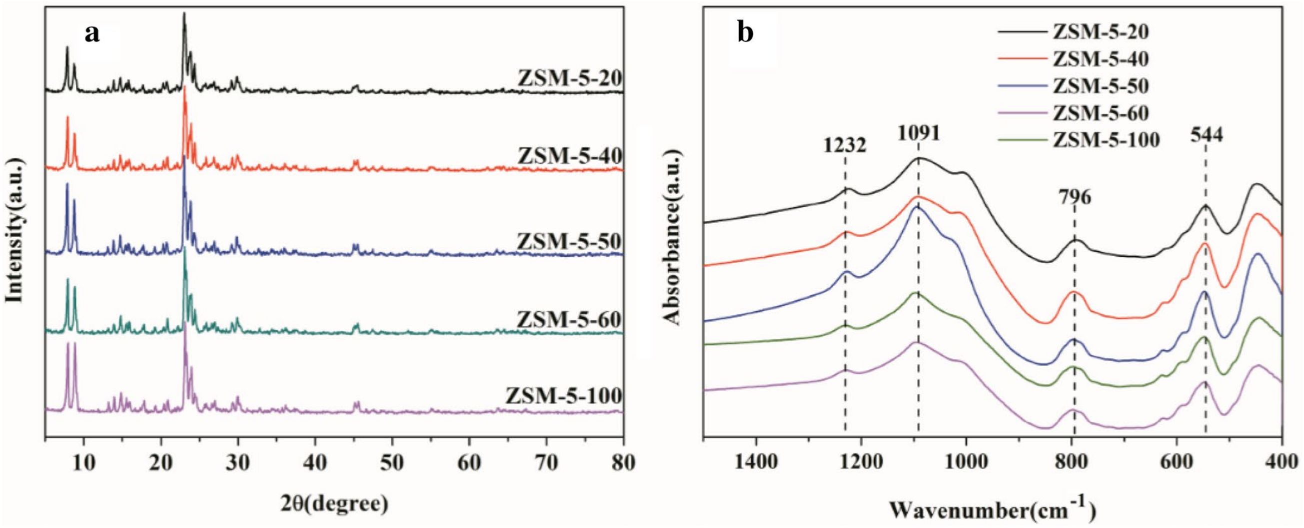

Fig. 1 XRD patterns (**a**) and FTIR spectra (**b**) of ZSM-5 with different silica/alumina molar ratios

Table 1 The characteristics of porous structure of ZSM-5 with different silica/alumina ratios

Sample	SiO_2/Al_2O_3 ratio[a]	S_{BET} (m^2/g)	Total pore volume (cm^3/g)	t-plot			Horvath-Kawazoe	
				S_{micro} (m^2/g)	$S_{external}$ (m^2/g)	V_{micro} (cm^3/g)	V_{micro} (cm^3/g)	W_{micro} (nm)
ZSM-5-20	23.32	280.75	0.176	221.34	59.41	0.118	0.142	0.636
ZSM-5-40	48.99	296.18	0.171	213.41	82.77	0.114	0.148	0.640
ZSM-5-50	60.51	307.03	0.176	212.65	94.76	0.114	0.153	0.658
ZSM-5-60	69.99	281.60	0.165	183.82	97.78	0.099	0.139	0.666
ZSM-5-100	113.56	305.35	0.165	201.19	104.16	0.107	0.150	0.670

[a] The silica/alumina molar ratio in zeolites was determined by X-ray fluorescence

S_{micro}: micropore surface area; $S_{external}$: specific surface area of mesopores and macropores ($S_{micro}+S_{external}=S_{BET}$); V_{micro}: micropore volume; W_{micro}: average width of micropores

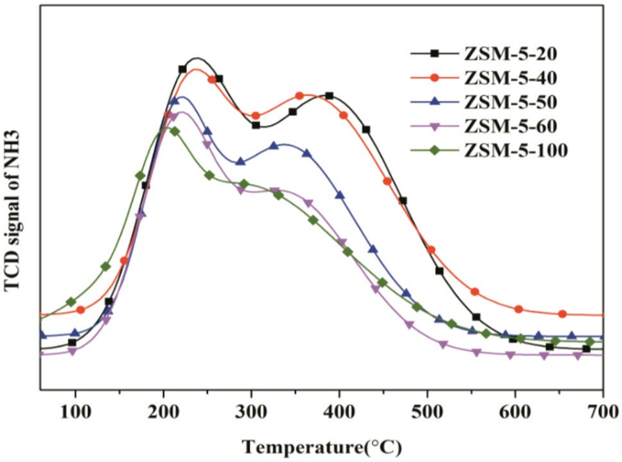

Fig. 3 NH_3-TPD profiles of ZSM-5 zeolites with different SiO_2/Al_2O_3 ratios

Table 2 The acid properties of ZSM-5 zeolites with different SiO_2/Al_2O_3 ratios according to NH_3-TPD

Sample	T_{peak} (°C)		Acid amounts based on NH_3-TPD data[b]		
	LT[a] peak	HT[a] peak	Weak	Strong	Total
ZSM-5-20	239	387	0.55	0.98	1.53
ZSM-5-40	237	356	0.33	0.91	1.24
ZSM-5-50	220	339	0.29	0.71	1.0
ZSM-5-60	218	335	0.35	0.60	0.95
ZSM-5-100	204	310	0.13	0.79	0.92

[a] The LT peak represents the low temperature desorption peak, the HT peak represents the high temperature desorption peak

[b] The total acid amount of ZSM-5-50 was assigned as 1.0 and the other samples were compared to ZSM-5-50

The effect of the ratio of silica to alumina in ZSM-5 zeolite on its acidity was studied by temperature-programmed desorption of ammonia (NH_3-TPD). As shown in Fig. 3, all of the samples display a similar TPD profile with two desorption peaks. The low-temperature desorption peak (LT peak) centered in a temperature range of 204–239 °C corresponds to the weak acid sites and the high-temperature desorption peak (HT peak) in the range of 310–387 °C corresponds to the strong acid sites. The LT peak is attributed to the adsorption of ammonia on the non-framework Al or the non-acid terminal Si–OH groups, similar to the silanol groups of silica [25]. As shown in Table 2, the amount of acidic sites is calculated by the area of desorbed ammonia. As the ratio of silica/alumina increases, the total acid amount decreases, while the amount of strong acid and weak acid also decreases. The decrease in acid amount is due to the decrease of Al in the framework as the ratio of silica to alumina increases, resulting in a decrease of Si–OH–Al [26]. In addition, with increasing silica/alumina ratio, it can been seen that both the LT peak and HT peak have a tendency to shift toward the lower temperature. This should be due to a decrease in the aluminum content of the sample, resulting in the weakening of the acidity of the sample [27].

The py-FTIR was used to analyze the Lewis acid sites (LAS) and Brønsted acid sites (BAS) on the surface of the sample. The spectrum in the range of 1400–1600 cm^{-1} indicate the type and relative amount of acid sites on the surface of the sample. Generally, the band at 1540 cm^{-1} can be attributed to the pyridine cation and indicates BAS, while the band at 1450 cm^{-1} is characteristic of pyridine coordinated to LAS [28]. The band at 1490 cm^{-1} is assigned to pyridine on both LAS and BAS. The amounts of LAS and BAS were calculated by the following Eqs. (1, 2).

$$C(\text{pyridine on acid sites}) = \frac{B\ \times\ \text{sample surface area}}{\text{adsorption cofficient} \times\ \text{mass}} \tag{1}$$

$$\text{B(band area)} = I_{\text{max}} W_{1/2} \tag{2}$$

where I_{max} is the intensity of the band (in absorbance unit), $W_{1/2}$ is half width at half height, mass denotes that of adsorbent. The adsorption coefficient of Lewis is 3.80, the adsorption coefficient of Brønsted is 3.03 [29]. Units of adsorption coefficient, mass, *B*, and sample surface area are cm $mmol^{-1}$, g, cm^{-1}, and cm^2, respectively. In ZSM-5 zeolite, BAS are formed by acidic Si–OH–Al groups [30, 31]. Dehydration of ZSM-5 zeolite at high temperature causes the tetracoordinated aluminum atom to lose an oxygen, forming a tricoordinated aluminum atom with an empty electron orbit, which is the formation of LAS [25]. In addition, the LAS is also related to non-framework aluminum in ZSM-5. The results of pyridine adsorption at 50 °C (see supporting information, Fig. S2 and Table S1) show that the total acid amount decreases with the increase of the ratio of silica to alumina, which was consistent with the NH_3-TPD results. The results of py-FTIR at 300 °C are shown in Fig. 4 and Table 3, representing the strong LAS and BAS amount of the ZSM-5 catalyst. In propylene oxide rearrangement, strong LAS is the active site for the formation of propionaldehyde [5, 18, 32]. But strong LAS and BAS are also related to the carbon deposition [33]. That is to say, the ratio of LAS to BAS has an important relationship with the conversion and stability of propylene oxide rearrangement. As the ratio of silica to alumina increases, the ratio of the amount of LAS to BAS first increases and then decreases, ZSM-5-50 has the largest ratio. Therefore, the ZSM-5-50 catalyst with the largest LAS to BAS ratio and the least amount of strong LAS and BAS showed the best catalytic performance.

Table 3 Surface acidities of adsorbents determined by pyridine adsorption

Sample	Amount of BAS (mmol g^{-1})	Amount of LAS(mmol g^{-1})	L/B
ZSM-5-20	8.00	8.90	1.11
ZSM-5-40	2.96	3.56	1.20
ZSM-5-50	0.1	1.86	18.6
ZSM-5-60	0.46	3.10	6.74
ZSM-5-100	2.74	0.11	0.04

3.2 LAS-Catalyzed Propylene Oxide Rearrangement

The in-situ DRIFTS technique was employed to study the adsorption and reaction behavior of propylene oxide on the ZSM-5-50 catalyst at reaction temperature. Figure 5 shows the spectra of ZSM-5-50 catalyst at different times after the introduction of propylene oxide. It can be seen from Fig. 5 that the intensity of the peak at 1685 cm^{-1} is increase greatly within 1.1 min and begins to decrease rapidly after 1.1 min, especially after 3.2 min. While the peak at 1719 cm^{-1} attributed to the carbonyl of propionaldehyde [34] is weaker at first and after 3.2 min stronger than that at 1685 cm^{-1}. It also increases within 1.1 min and after 3.2 min begins to fade away slowly. The peak at 1685 cm^{-1} disappears completely at 8.5 min but that at 1719 cm^{-1} still exists at 18.6 min. This strongly implies that the structure at 1685 cm^{-1} precedes the formation and disappearance of the carbonyl group. As comparison, the same in-situ DRIFTS experiment was carried out using silica as the catalyst under the same conditions. The spectra (as shown in supporting information, Fig. S3) shows only a weak peak at 1725 cm^{-1} which is attributed to carbonyl which is due to thermal rearrangement of propylene oxide at 300 °C rather than catalytic rearrangement [6]. This indicates that the generation of the peak at 1685 cm^{-1} is related to the Al atom in the ZSM-5 catalyst, that is, the Lewis acid site. It is the conjugation of Al atom and the the cleavage –C–O of the epoxy ring (i.e., C=O precursor) before the formation of the carbonyl group [35–37].

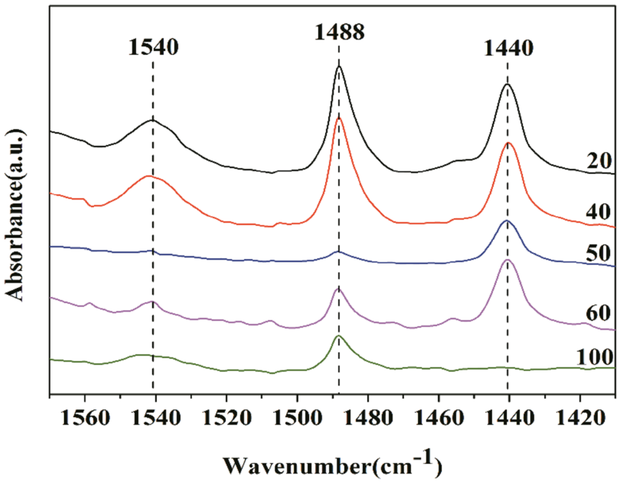

Fig. 4 Pyridine adsorption IR spectra of ZSM-5 with different SiO_2/Al_2O_3 ratios at 300 °C

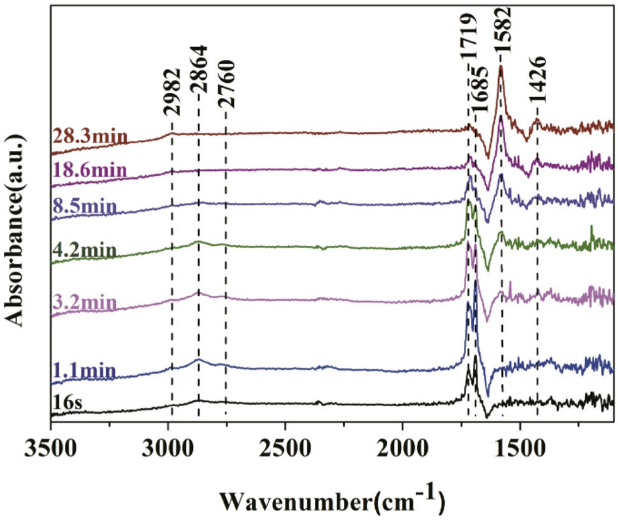

Fig. 5 Evolution of DRIFT spectra for propylene oxide adsorption on ZSM-5-50 at 300°C

In addition, the peaks at 2864 cm^{-1} and 2760 cm^{-1} in Fig. 5 are attributed to C–H stretching vibration of aldehyde group, and the peak at 2982 cm^{-1} attributed to C–H stretching vibration of alkyl group [38, 39]. As the peak at 1719 cm^{-1} gradually decreases, the peaks of 1582 cm^{-1} and 1426 cm^{-1} begin to appear and increase significantly. We conclude that it should be the vibrational peaks of C=C and C–C bonds, respectively, which is of a precursor of carbon deposits [40].

According to the results of in-situ DRIFTS, we propose the mechanism of propylene oxide rearrangement to propionaldehyde as shown in Fig. 6. Under the catalysis of Lewis acid, the oxygen atom in the epoxy ring adsorbs on the aluminum atom, resulting in the cleavage of the a–C–O bond. At the same time, along with hydrogen transfer, the intermediate of C⋯O which is between C=O bond and C–O bond or closer to C=O is formed. The peak at 1685 cm^{-1} is assigned to the intermediate structure C⋯O, which is the precursor of C=O. After the a–C–O cleavage, the carbonyl group has not yet formed, the carbon–oxygen double bond of the intermediate structure is weak, resulting in its appearance at 1685 cm^{-1}. Finally, the intermediate structure quickly converts to propionaldehyde.

3.3 Catalytic Activity, Stability and Acidity

The conversion and product selectivity of propylene oxide rearrangement catalyzed by ZSM-5 catalysts with different ratios of silica to alumina are shown in Fig. 7. It can be clearly seen that the ratio of silica to alumina of ZSM-5 catalyst has a great influence on the conversion and the stability. The initial conversion of ZSM-5-20 catalyst reached 80%, but it deactivated very sharply. The conversion decreased to about 20% after 2 h, as the ZSM-5-20 catalyst had the highest total amount of strong acid, which leads to rapid carbon deposition. The ZSM-5-40 and ZSM-5-60 catalysts have the same amounts of LAS, but the ZSM-5-60 catalyst has fewer BAS than ZSM-5-40. Therefore, they all have a high initial conversion and the ZSM-5-60 catalyst has better stability than ZSM-5-40. The conversion of the ZSM-5-100 catalyst in the initial stage is very low and always remains below 20%. It is precisely because of the small amount of strong LAS that it is insufficient to provide the active sites required for the reaction. For the catalyst ZSM-5-50 with the highest LAS to BAS ratio and the lowest total amount of strong acid site, the conversion remained above 90% for 8 h. It can been seen from Fig. 7b that as the ratio of silica to alumina increases, the selectivity of propionaldehyde first increases and then decreases. Combined with the pyridine adsorption results at 300 °C, the change tendency of propionaldehyde selectivity is the same as the change tendency of the ratio of the amount of LAS to BAS. The ZSM-5-50 catalyst has the largest ratio of the amount of LAS to BAS and also has the highest selectivity to propionaldehyde, about 93%. We can conclude that when ZSM-5 catalyzes the rearrangement of propylene oxide to propionaldehyde, the conversion, stability and selectivity are proportional to the ratio of LAS to BAS at 300 °C. That is to say, the larger the ratio, the higher the conversion and selectivity of propionaldehyde, and the smaller the total amount of LAS and BAS, the better the stability of the catalyst.

The stability of catalysts for the rearrangement of propylene oxide is always a problem and is rarely reported in previous studies. Here the stability test of ZSM-5-50 catalyst was carried out at 300 °C with a WHSV of 19 h^{-1} as shown

Fig. 6 The mechanism diagram of propylene oxide rearrangement to propionaldehyde

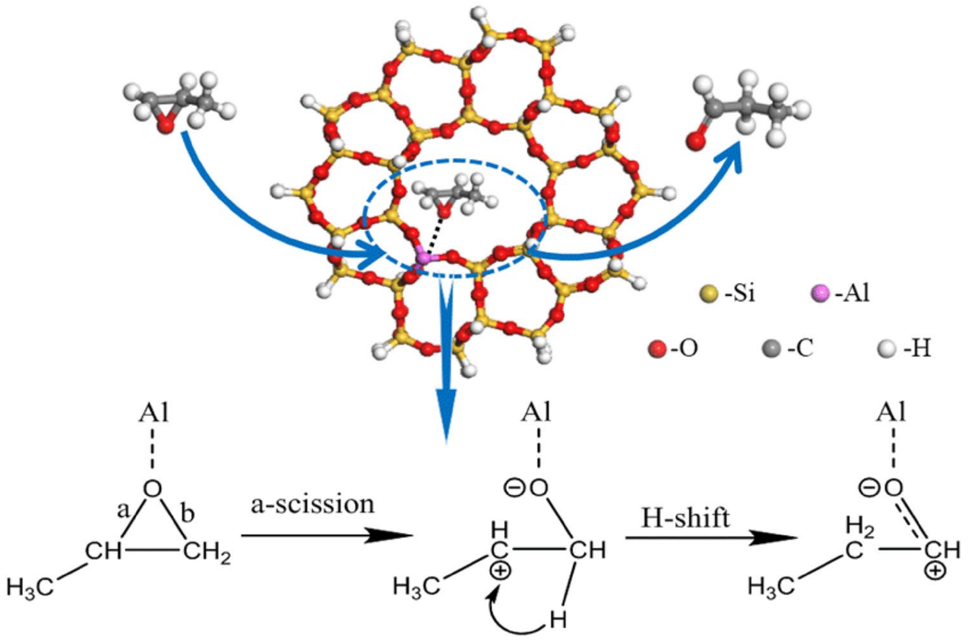

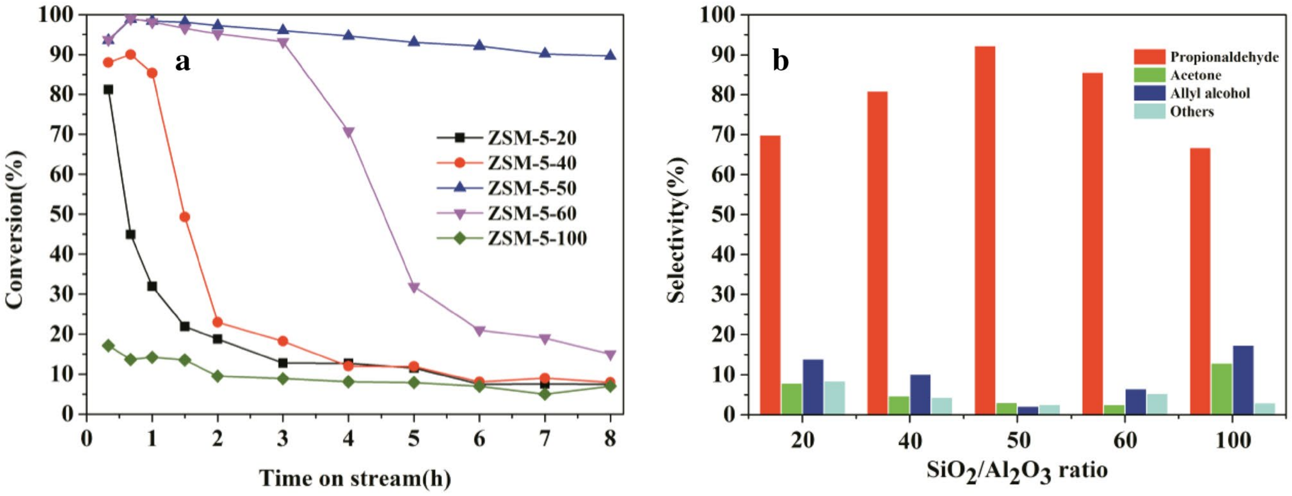

Fig. 7 The conversion of propylene oxide rearrangement (**a**) and the product selectivity (**b**)

in Fig. 8a. It is clearly seen that ZSM-5-50 catalyst is able to maintain its catalytic stability within 35 h, with only a slight decline. The conversion at the reaction time of 35 h is still above 90% with selectivity of as high as 85% for propionaldehyde. The slight decrease of the conversion and the selectivity may be ascribed to the inevitable carbon deposition, which is a common problem for the acid-base catalysts. As shown in Fig. 8b, both the fresh and used catalysts show weight loss below 200 °C due to the removal of moisture [41], while the used catalyst experienced another weight loss procedure in the temperature range of 300–500 °C which should be attributed to the decomposition of carbonaceous deposits (0.12 g/g_{cat}) [42]. Compared with previous studies on the stability and carbon deposition of catalyst, ZSM-5-50 has better stability and less carbon deposit [4, 40].

4 Conclusions

We investigated the effect of the silica/alumina ratio on the acidity of ZSM-5 zeolite and its effect on the propylene oxide rearrangement. For the ZSM-5 catalysts, the change of silica/alumina ratio has slight effects on physical properties such as morphology, specific surface area and pore volume. However, the change of silica/alumina ratio significantly affects the acidity of ZSM-5. With the increase of silica/alumina ratio, the total acid amount decreases and the acid strength becomes weaker, the decrease of Al atom content in ZSM-5 is the primary cause of acidity change. The results of Py-FTIR on the catalyst show that the ratio of the amount of LAS to BAS increases first

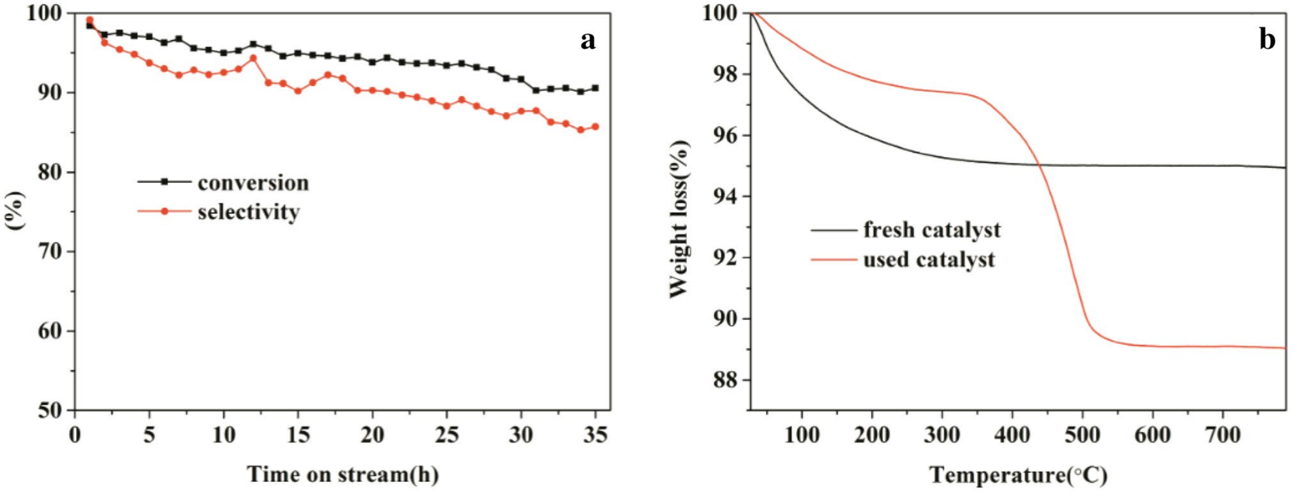

Fig. 8 Stability test over ZSM-5-50 catalyst with time on stream (**a**) and thermal gravity curves of fresh and used ZSM-5-50 catalyst (**b**)

and then decreases with the increase of the ratio of silica/alumina, and the change of this ratio directly affect the catalytic performance of the catalyst. The larger the ratio, the better the catalytic performance. The lower the total amount of LAS and BAS at reaction temperature, the better the stability of the catalyst. The catalyst ZSM-5-50 with the highest LAS to BAS ratio and the least amount of LAS and BAS has the best conversion and propionaldehyde selectivity. Finally, the mechanism of rearrangement of propylene oxide on ZSM-5 catalyst was investigated by in-situ DRIFTS technique. We conclude that the oxygen atom in the epoxy ring of propylene oxide first adsorbs aluminum atom containing an empty electron orbital in the ZSM-5 catalyst. Then an intermediate is formed with the bond between C=O and C–O and finally converts to the target product propionaldehyde.

Acknowledgements This work was supported by the National Natural Science Foundation of China (No. 21276127).

Compliance with Ethical Standards

Conflict of interest The authors declare that they have no conflict of interest.

References

1. Barreca D, Copley MP, Graham AE, Holmes JD, Morris MA, Seraglia R, Spalding TR, Tondello E (2006) Appl Catal A 304:14–20
2. Smith BM, Skellam EJ, Oxley SJ, Graham AE (2007) Org Biomol Chem 5:1979–1982
3. Smith K, El-Hiti GA, Al-Shamali M (2006) Catal Lett 109:77–82
4. Wang Y, Li Z, Ma W, Kinnuda G, Qu H, Zhong Q (2016) Rsc Adv 6:57000–57008
5. Serrano DP, Grieken RV, Melero JA, García A, Vargas C (2010) J Mol Catal A 318:68–74
6. Wang Y, Ma W, Wang D, Zhong Q (2017) Chem Eng J 307:1047–1054
7. Zhang J, Wang D, Ma W (2017) Nano Brief Rep Rev 13:1
8. Ma W, Si W, Wu W, Zhong Q (2011) Catal Lett 141:1032–1036
9. Smith K, El-Hiti GA, Matthews I, Al-Shamali M, Watson T (2009) Catal Lett 128:101–105
10. Lan DH, Wang HT, Chen L, Au CT, Yin SF (2016) Carbon 100:81–89
11. Mao J, Wang Y, Zhu J, Yu J, Hu Z (2018) Appl Surf Sci 447:235–243
12. Zhang Z, Sun X, Zhang X, Fang X (2016) Catal Lett 146:1–7
13. Ishihara K, Hanaki N, Yamamoto H (2010) Cheminform 26:225–230
14. Suda K, Nakajima SI, Satoh Y, Takanami T (2009) Chem Commun 40:1255–1257
15. Raptis C, Garcia H, Stratakis M (2010) Angew Chem Int Ed 48:3133–3136
16. Serrano DP, Uguina MA, Ovejero G, Grieken RV, Camacho M (1995) Microporous Mater 4:273–282
17. Zhang XF, Yao J, Yang X (2017) Catal Lett 147:1–10
18. Virnig MJ (1991) Process for isomerizing epoxides to ketones US 5032323
19. Hoelderich W, Goetz N, Hupfer L, Lermer H (1990) Preparation of aldehydes and/or ketones BU conversion of epoxides US 4980511
20. Wu Z, Liu S, Xie S, Wang Q, Qian X, Xu L (2005) React Kinet Catal Lett 84:45–51
21. Mei C, Wen P, Liu Z, Liu H, Wang Y, Yang W, Xie Z, Hua W, Gao Z (2008) J Catal 258:243–249
22. Serrano DP, Sanz R, Pizarro P, Moreno I, Medina S (2014) Appl Catal B 146:35–42
23. Feng X, Sheng N, Liu Y, Chen X, Chen D, Yang C, Zhou X (2017) Acs Catal 7:2668–2675
24. Jiang X, Su X, Bai X, Li Y, Yang L, Zhang K, Zhang Y, Liu Y, Wu W (2017) Microporous Mesoporous Mater 263:243–250
25. Kolobova E, Pestryakov A, Mamontov G, Kotolevich Y, Bogdanchikova N, Farias M, Vosmerikov A, Vosmerikova L, Corberan VC (2017) Fuel 188:121–131
26. Gao Y, Wu G, Ma F, Liu C, Jiang F, Wang Y, Wang A (2016) Microporous Mesoporous Mater 226:251–259
27. Shirazi L, Jamshidi E, Ghasemi MR (2010) Cryst Res Technol 43:1300–1306
28. Yue Y, Gu L, Zhou Y, Liu H, Yuan P, Zhu H, Bai Z, Bao X (2017) Ind Eng Chem Res 56:10069–10077
29. Farneth WE, Gorte RJ (1995) Chem Rev 95:615–635
30. Brus J, Kobera L, Schoefberger W, Urbanová M, Klein P, Sazama P, Tabor E, Sklenak S, Fishchuk AV, Dědeček J (2015) Angew Chem Int Ed Engl 127:551–555
31. Yarulina I, De KW, Bailleul S, Goetze J, Radersma M, Abou-hamad E, Vollmer I, Goesten M, Mezari B, Hensen E (2018) Nat Chem 10:1
32. Li JJ (2003) Meinwald rearrangement. Springer, Berlin
33. Müller S, Liu Y, Vishnuvarthan M, Sun X, Veen ACV, Haller GL, Sanchez-Sanchez M, Lercher JA (2015) J Catal 325:48–59
34. Tan J, Cui J, Cui X, Deng T, Li X, Zhu Y, Li Y (2015) Acs Catal 5(12):7379–7384
35. Shlykov SA, Phien TD, Trang NH (2017) Tetrahedron 73(35):5311–5320
36. Sajan D, Lakshmi KU, Erdogdu Y, Joe IH (2011) Spectrochim Acta A 78:113–121
37. Sajan D, Joe IH, Jayakumar VS (2010) J Raman Spectrosc 37:508–519
38. Ying M, Zhang G (2016) Chem Eng J 288:70–78
39. Jetzki M, Luckhaus D, Signorell R (2004) Rev Can Chim 82:915–924
40. Jiang L, Li H, Wang Y, Ma W, Zhong Q (2015) Catal Commun 64:22–26
41. Zhang X, Lin L, Zhang T, Liu H, Zhang X (2016) Chem Eng J 284:934–941
42. Zhang G, Zhang X, Bai T, Chen T, Fan W (2015) J Energy Chem 24:108–118

Publisher's Note Springer Nature remains neutral with regard to jurisdictional claims in published maps and institutional affiliations.